Journal of the Pediatric Infectious Diseases Society

ORIGINAL ARTICLE

Transient Viral Rebound in Children with Perinatally Acquired HIV-1 Induces a Unique Soluble Immunometabolic Signature Associated with Decreased CD4/CD8 Ratio

Laura Tarancon-Diez[1,#], Joaquim Peraire[#,2,3,4,5], Santiago Jiménez de Ory[5,6], Maria Guirro[7], Luis Escosa[5,8], Luis Manuel Prieto Tato[9], María Penín Antón[10], Ana Isabel Piqueras[11], Álvaro Vázquez Pérez[12], César Gavilán[13], Matilde Bustillo-Alonso[14], María Luisa Navarro[5,6,15], Consuelo Viladés[2,3,4,5], Francesc Vidal[2,3,4,5], Anna Rull[2,3,4,5,†], and María Ángeles Muñoz-Fernández[1,16,†]

[1]Molecular Immunology Laboratory, Hospital General Universitario Gregorio Marañón, Health Research Institute Gregorio Marañón (IiSGM), Madrid, Spain, [2]Universitat Rovira i Virgili, Tarragona, Spain, [3]Institut Investigació Sanitària Pere Virgili (IISPV), Tarragona, Spain, [4]Hospital Universitari de Tarragona Joan XXIII, Tarragona, Spain, [5]Centro de Investigación Biomédica en Red de Enfermedades Infecciosas (CIBERINFEC), Instituto de Salud Carlos III (ISCIII), Madrid, Spain, [6]Grupo de Infecciones en la Población Pediátrica, Instituto de Investigación Sanitaria Gregorio Marañón, Madrid, Spain, [7]Centre for Omic Sciences, Eurecat, Centre Tecnològic de Catalunya (Joint Unit Eurecat-Universitat Rovira i Virgili), Unique Scientific and Technical Infrastructure (ICTS), 43204 Reus, Spain, [8]Servicio de Pediatría, Enfermedades Infecciosas y Tropicales, Hospital Universitario La Paz y La Paz Research Institute (IdiPAZ), Hospital Universitario La Paz, Madrid, Spain, [9]Servicio de Pediatría, Hospital Universitario 12 de Octubre e Instituto de Investigación I+12, 28041, Madrid, Spain, [10]Servicio de pediatría, Hospital Universitario Príncipe de Asturias, Alcalá de Henares, Spain, [11]Pediatric Infectious Diseases Unit, Hospital Universitario y Politécnico La Fe, Hospital La Fe, Valencia, Spain, [12]Department of Pediatrics, Virgen de las Nieves Children's Hospital, Granada, Spain, [13]Servicio de Pediatría, Hospital San Juan de Alicante, Sant Joan d'Alacant, Spain, [14]Servicio de Pediatría. Enfermedades Infecciosas, Hospital Universitario Miguel Servet, Zaragoza, Spain, [15]Servicio de Pediatría, Hospital General Universitario Gregorio Marañón, Madrid, Spain, and [16]Centro de Investigación Biomédica en Red de Bioingeniería, Biomateriales y Nanomedicina (CIBER-BBN), Instituto de Salud Carlos III (ISCIII), Madrid, Spain

Background. To determine by multi-omic analysis changes in metabolites, lipids, and proteins as a consequence of transient viral rebound (tVR) in children with perinatally acquired HIV-1 (PHIV).

Methods. Plasma samples from children with PHIV and with tVR (first episode of transient RNA-HIV viral load >20 copies/ml followed by suppression) on the time-point immediately before (pre-tVR) and after (post-tVR) the tVR were assessed. Multi-omic analyses were performed using nLC-Orbitrap, GC-qTOF-MS, and LC-qTOF-MS.

Results. Comparing pre- and post-tVR time-points, HIV-1 children with tVR ($n = 5$) showed a trend to a decrease in ratio CD4/CD8 ($p = 0.08$) but no significant differences were observed in plasma metabolites, lipids, or proteins. Post-tVR condition was compared with a reference group of children with PHIV with persistent viral control ($n = 9$), paired by sex, age, and time under antiretroviral treatment. A total of 10 proteins, 8 metabolites, and 2 lipids showed significant differences ($p < 0.05$): serotransferrin, clusterin, kininogen-1, succinic acid, threonine, 2-hydroxyisovaleric acid, methionine, 2-hydroxyglutaric, triacylglyceride 50:0 (TG50:0), and diacylglyceride 34:1 (DG34:1) were upregulated while alpha-2-macroglobulin, apolipoprotein A-II, carboxylic ester hydrolase, apolipoprotein D, coagulation factor IX, peptidase inhibitor 16, SAA2-SAA4 readthrough, oleic acid, palmitoleic acid, and D-sucrose downregulated on post-tVR time-point compared to the reference group. Ratio CD4/CD8 correlated with apolipoprotein A-II, DG34:1, and methionine ($p = 0.004$; $\rho = 0.71$, $p = 0.016$; $\rho = -0.63$; and $p = 0.032$; $\rho = -0.57$, respectively). Nadir CD4+ correlated inversely with kininogen-1 ($p = 0.022$; $\rho = -0.60$) and positively with D-sucrose ($p = 0.001$; $\rho = 0.77$).

Conclusions. tVR followed by suppression implies changes in soluble proteins, lipids, and metabolites that correlate with immunological parameters, mainly ratio CD4/CD8, that decreased after tVR. These distinct soluble biomarkers could be considered potential biomarkers of immune progression.

Key words. omics; ratio CD4/CD8; vertically HIV-1 children; viral rebounds.

Received 4 November 2022; editorial decision 25 January 2023; accepted 31 January 2023; published online 2 February 2023

[#]These authors have contributed equally to this work and share first authorship.

[†]These authors have contributed equally to this work and share senior authorship.

Corresponding Author: Anna Rull, PhD, Institut Investigació Sanitària Pere Virgili (IISPV), Tarragona, Spain. E-mail: anna.rull@iispv.cat.

Journal of the Pediatric Infectious Diseases Society 2023;12(3):143–51

https://doi.org/10.1093/jpids/piad008

INTRODUCTION

The purpose of antiretroviral treatment (ART) is to achieve long-term maintenance of suppressed HIV-1 viral load during chronic infection. Although this is achieved in the majority of patients, some of them experience viral rebounds over time. Viral rebounds are defined as transient, low-level detectable viral load. Despite the fact that transient viral rebounds (tVR) are common during ART, the mechanistic pathways, consequences, and optimal management remain still unclear. Proposed explanations for tVR include drug resistance development [1],

fluctuations or lack of ART adherence [2], concurrent illnesses [3], and concerning blips, they may represent residual low-level viral replication that may sometimes lead to virologic failure [4–6]. However, among the consequences, the probably gradual rise in the risk of viral failure with increasing viral replication magnitude [7, 8] and the changes in immune activation profile before, during, and after tVR show certain discrepancies in the literature [9, 10]. All the described above has been observed in HIV-1-infected adults, but in children with perinatally acquired HIV-1 (PHIV), tVR has also been associated with drug failure and lack of adherence [11–13], and late ART introduction [14].

Most efforts up to the moment have been focused on analyzing the incidence of viral rebounds, its association with clinical and epidemiological variables [15] and on identifying immunological predictors of spontaneous blips or loss of control after treatment interruption in vertically HIV-1 adults and adolescents [16], but there are scarce data on the clinical and immunometabolic outcomes following tVR in children with PHIV.

HIV-1 infection causes up-regulation of glucose, lipids, and tryptophan and cell oxidative stress that ultimately dampens the protective response of both innate and adaptive arms of immunity [17, 18]. Whether tVR may imply also irreversible changes in the metabolic profile even after viral suppression recovery remains unknown. The objective of this work was to determine by multi-omic analysis the changes in soluble metabolites, lipids, and proteins associated with tVR in children with PHIV to gain further immunometabolic insights related to HIV-1 infection.

METHODS

Study Participants and Design

Participants for this retrospective analysis of prospectively collected patients and data were children and adolescents with PHIV selected from the Paediatric Spanish AIDS Research Network Cohort (coRISpe) and evaluated approximately every 6–12 months [19]. All participants were younger than 18 years old and achieved viral load suppression when on ART. Exclusion criteria were: (1) previous or current hepatitis C virus and/or hepatitis B virus co-infections; (2) inflammatory or metabolic diseases; and (3) medications except for ART. To analyze the consequences of short-time increased viral replication with soluble biomarkers and immunological variables, patients were divided into two groups, based on the presence or absence of tVR control followed by viral suppression: a group with tVR (n = 5) (see details in Table 1) and persistent viral control group (n = 9) (see details in Table 2). Causes of tVR include blips (transient RNA-HIV viral load values above the detection limit, >20 copies/ml, but less than 1000 copies/ml, with the return to viral suppression without a change in therapy) and viral failure (transient RNA-HIV viral load values above 1000 copies/ml due to therapy failure or lack of adherence followed by viral suppression after treatment replacement or reimplementation). In the loss of viral control group (n = 5), the first episode of tVR was evaluated per patient and the inclusion criteria for that group included repository plasma sample available on the Spanish HIV BioBank [20] on the dates immediately before (pre-tVR) and after (post-tVR) the increased viral load, being for both time-points the RNA-HIV below the detection limit. Only one time-point with available plasma sample was evaluated from patients belonging to the group of persistent viral control. This group was paired by age, sex, and time under ART with the group of children with tVR and used as a reference group for all comparisons.

The study was approved by the ethics committee of Hospital General Universitario Gregorio Marañón (HGUGM) in Madrid (protocol miRNA-Ped-HIV_16, approved on March 21, 2017, acta06/2017). Written informed consent was obtained from all children's parents or guardians.

Table 1. General Characteristics of Children with Perinatally Acquired HIV-1 with tVR at Study Enrollment and Immunological, Virological and Biochemical Parameters at Pre- and Post-transient Virologic Rebound

General characteristics	Patient 1		Patient 2		Patient 3		Patient 4		Patient 5	
Sex	Male		Female		Male		Female		Female	
Age at ART initiation (wk)	240		36		92		8		32	
Nadir CD4+ cells/mm3	230		393		418		310		707	
RNA-HIV copies/ml at tVR	264		1300		22,125		5040		486	
Causes of viral rebound	Spontaneous blip		Viral failure		Viral failure		Lack of adherence		Spontaneous blip	
Parameters at sampling	**Pre-tVR**	**Post-tVR**	**Pre-tVR**	**Post-tVR**	**Pre-tVR**	**Post-tVR**	**Pre-tVR**	**Post-tVR**	**Pre-tVR**	**Post-tVR**
Age (years)	9	11	11	12	10	12	9	11	4	5
Time since ART initiation (wk)	240	na	537	na	444	na	492	na	176	na
Time under virologic control (months)	56	na	128	na	108	na	98	na	42	na
n CD4+ cells/mm3	370	330	1545	564	905	979	1009	632	1720	1416
n CD8+ cells/mm3	600	530	1142	615	416	593	337	391	983	1463
CD4+/CD8+	0.62	0.62	1.35	0.92	2.18	1.65	2.99	1.62	1.75	0.97

Abbreviations: ART, antiretroviral therapy; na, no applicable; tVR, transient viral rebound; wk, weeks. Blips are defined as transient VL values above detection limit, >20 copies/ml, but less than 1000 copies/ml, with return to viral suppression without a change in therapy. Viral failure is defined as transient VL values above 1000 copies/ml due to lack of adherence followed by viral suppression after treatment replacement or reimplementation.

Table 2. Participants' Characteristics of the Group of Children with Perinatally Acquired HIV-1 with tVR Compared to a Group of Children HIV-1 Children with Persistent Control

	Children with PHIV with tVR ($n = 5$)	Children with PHIV with persistent viral control ($n = 9$)	p
Subject characteristics			
Sex (male) *n* (%)	2 (40)	2 (22)	0.480
Nadir CD4+ cells/mm^3	393 [270–562]	727 [435–966]	0.072
Age at ART initiation (wk)	36 [20–166]	7 [1.5–18.5]	**0.014**
Parameters at sampling			
Age (years)	11 [8–12]	9 [7–10.5]	0.252
Time since ART initiation (months)	124 [67.5–142]	114 [87–132]	0.947
%CD4+	32.2 [23.8–39]	42 [39–45.6]	**0.038**
n CD4+ cells/mm^3	632 [447–1197]	976 [875–1148]	0.317
%CD8+	33.3 [21.5–37]	23 [20.2–26.1]	0.082
n CD8+ cells/mm^3	593 [460–1039]	574 [400–700]	0.549
CD4+/CD8+	0.97 [0.77–1.63]	1.83 [1.72–2.21]	**0.006**
Biochemical parameters			
Glucose (mg/dl)	81 [47.5–83.5]	83 [79–91.5]	0.204
GPT (ALT) U/L	20 [15–46]	17.5 [10.25–24.5]	0.272
GOT (AST) U/L	23 [11.8–33.5]	32 [26–35]	0.291
Total cholesterol (mg/dl)	185 [176–211]	174 [162–195]	0.161
Triglycerides (mg/dl)	72 [39–135]	80 [56–105.5]	0.548
LDL (mg/dl)	100 [49.2–123]	97 [85–128]	0.769
HDL (mg/dl)	60 [31–66.5]	63 [56.5–68]	0.304
LDL/HDL	1.63 [0.72–2.77]	1.39 [1.36–2.09]	0.661
Creatinine (mg/dl)	0.44 [0.43–0.5]	0.5 [0.46–0.57]	0.228

Abbreviations: PHIV, perinatally acquired HIV-1, tVR, transient viral rebound; ART, antiretroviral therapy; GPT, glutamate pyruvate transaminase; ALT, alanine aminotransferase; GOT, glutamic oxaloacetic transaminase; AST, aspartate aminotransferase; LDL, low-density lipoprotein cholesterol; HDL, high-density lipoprotein cholesterol. Parameters at sampling from children with PHIV with tVR are taken at post-tVR time-point (post-tVR). Values are showed as median [interquartile range] for continuous variables or numbers (%) for categorical variables. Mann–Whitney test and chi-square test were used for comparisons between continuous and categorical variables, respectively.

Laboratory Measurements

Blood was drawn from a peripheral vein after an overnight fast, collected in ethylenediaminetetraacetic acid (EDTA) tubes and plasma was isolated using a Ficoll density gradient and stored at −80°C at the Spanish HIV BioBank until further analysis.

Multi-omic Analyses (Extended Version on Supplementary Material)

Proteomics.

Thirty µg of depleted proteins were reduced and alkylated in dark. Afterward, samples were digested overnight (pH 8.0, 37°C) with sequencing-grade Trypsin/Lys-C Protease Mix (Thermo Fisher Scientific, CA, USA). Digestion was quenched by acidification with 1% (v/v) formic acid and peptides were desalted on Oasis HLB SPE column (Waters, Massachusetts, USA) before TMT 11-plex labeling (Thermo Fisher Scientific) following manufacturer instructions. The different TMT 11-plex batches were again desalted on Oasis HLB SPE columns before the nanoLC-MS analysis.

Labeled and multiplexed peptides were loaded on a trap nano-column (ThermoFisher Scientific, CA, USA) and separated onto a C18 reversed phase (RP) nano-column (Nikkyo Technos Co. LTD, Japan) on an EASY-II nanoLC from ThermoFisher. Mass spectrometry analyses were performed on an LTQ-Orbitrap Velos Pro from ThermoFisher by an enhanced FT-resolution MS spectrum (R = 30,000 FHMW) followed by a data-dependent FT-MS/MS acquisition (R = 15,000 FHMW, 40% NCE HCD).

Protein identification and quantification were performed on Proteome Discoverer software v.1.4.0.288 (Thermo Fisher) by Multidimensional Protein Identification Technology (MudPIT) combining the three raw data files obtained from each TMT plex. For protein identification, all MS and MS/MS spectra were analyzed using the Mascot search engine (v.2.5) combining the Homo Sapiens database (74449 entries) and the contaminants database (247 entries). For protein quantification, the ratios between each TMT-label against 126-TMT label were used and quantification results were normalized based on the protein median [21].

Metabolomics.

After protein precipitation, samples were mixed and incubated at 4°C for 10 min, centrifuged at 15,000 rpm and the supernatant was evaporated to dryness before derivatization. Samples were analyzed on a 7200 GC-QTOF from Agilent Technologies (Sta. Clara, CA, USA). Chromatographic separation was based on Fiehn Method, using a J&W Scientific HP5-MS. Ionization was performed by electronic impact and the mass analyzer was operated in full scan mode [21].

Targeted compounds were identified using pure standards, when available, with a mass accuracy of 20 ppm. The internal standards were used to correct signal response. Chromatographic peaks were deconvoluted using Unknowns Analysis software (version B.09.00, from Agilent) based on the exact mass. For compounds without a commercial standard, the tentative identification was made by comparing the mass spectra and retention time with the Fiehn 2013 Mass Spectral RTL Library and the National Institute of Standards and Technology (NIST) library 11 (2014) libraries also using the Unknowns software. After direct (with pure standards) or putative (with library) identification of metabolites, these were semiquantified in terms of internal standard response ratio.

Lipidomics.

For the extraction of the most hydrophobic lipidic fractions, a liquid-liquid extraction with chloroform:methanol based on the Folch procedure was performed. The organic phase was recovered, evaporated to dryness, and reconstituted before being analyzed on an Agilent 1290 Infinity UHPLC coupled to an Agilent 6550 qTOF mass spectrometer. The chromatographic separation consists of a ternary mobile phase. The stationary phase was a C18 column (Kinetex EVO C18 Column) that allows the sequential elution of the more hydrophobic lipids.

The identification of lipid species was performed using the Agilent MassHunter Profinder B.08 software. First, a feature extraction deconvolution was made; then accurate mass and tandem mass spectrum, when available, was matched to Metlin-PCDL (2017) from Agilent containing more than 40,000 metabolites and lipids, allowing a mass error of 20 ppm and a score higher than 80 for isotopic distribution. To ensure the tentative characterization, the chromatographic behavior of pure standards for each family and corroboration with the Lipid Maps database (www.lipidmaps.org) was used to ensure their putative identification. Afterward, matched entities were selected to perform a targeted MS/MS acquisition on the LC-QTOF-MS instrument to corroborate the identification. Then, lipid species were semiquantified in terms of internal standard response ratio using one internal standard for each lipid family.

The name of each compound is abbreviated as follows: CE for cholesteryl ester, DG for diacylglycerol, LPC for lysophosphocholine, PC for phosphatidylcholine, SM for sphingomyelin, and TG for triacylglycerol.

Statistical Analysis

Continuous variables were described as a median and interquartile range (IQR) and categorical variables as absolute numbers and percentages. Differences between categorical and continuous values were determined using the chi-square test and two-tailed Mann–Whitney U-test, respectively. The Spearman's rank test was used to analyze correlations between variables.

For multi-omic statistical analyses, only those proteins, lipids, and metabolites that were present at >60% of samples including both groups were considered. Missing value estimation after filtering was performed using the KNN algorism (k-nearest neighbors). A log base 2 transformation (Mass Profiler Professional software v. 14.5 from Agilent Technologies) was applied to omics data for variance stabilization, data range compression, and data normalization. Unpaired T-test was performed between tVR and reference groups and paired T-test between pre-tVR and post-tVR samples. For both comparisons, a p-value cut-off of < 0.05 and a fold-change cut-off of > 1.1 was applied. Multivariate analysis such as principal component analysis was performed from those significant proteins between comparisons.

The statistical software used was SPSS Software v22 and the web-based analytical MetaboAnalyst 5.0. Graphs were generated using GraphPad Prism 9.0., MetaboAnalyst 5.0, and Mass Profiler Professional software, as indicated in the figure legends. The results were considered statistically significant at p-value < 0.05.

RESULTS

Clinical and demographic characteristics of children with PHIV with tVR ($n = 5$) at study enrollment and immunological and biochemical parameters from both studied time points (pre-tVR and post-tVR) are shown in Table 1. Detailed ART-HIV regimens description at both time points is shown in Supplementary Table 1. None of the children had previous or current co-infection with Mycobacterium tuberculosis. Plasma HIV-RNA viral load and ratio CD4/CD8 evolution over time per child are represented in Figure 1. Children had a median follow-up of 12 years [IQR: 11–16] and the two analyzed follow-up time points were separated in time by a median of 23 months [IQR: 18–23.5]. Ratio CD4/CD8 comparison between pre-tVR and post-tVR showed a decrease in ratio CD4/CD8 that remained close to statistical significance ($p = 0.08$). No significant differences or trends were observed in the remaining variables.

Omic approaches identified and quantified 188, 81, and 115 plasma proteins, metabolites, and lipids, respectively. Comparing paired time-points, no significant differences in the relative abundance of proteins, metabolites, and lipids were observed between pre- and post-tVR.

Immunometabolic Signature Associated with Transient Viral Rebound (tVR)

After tVR, the post-tVR was compared with a reference group of children with PHIV with persistent viral control ($n = 9$) matched by sex, age at sampling, and time since ART initiation, for determining the possible consequences of tVR despite being followed by viral suppression. Clinical and immunological characteristics and biochemical and inflammatory

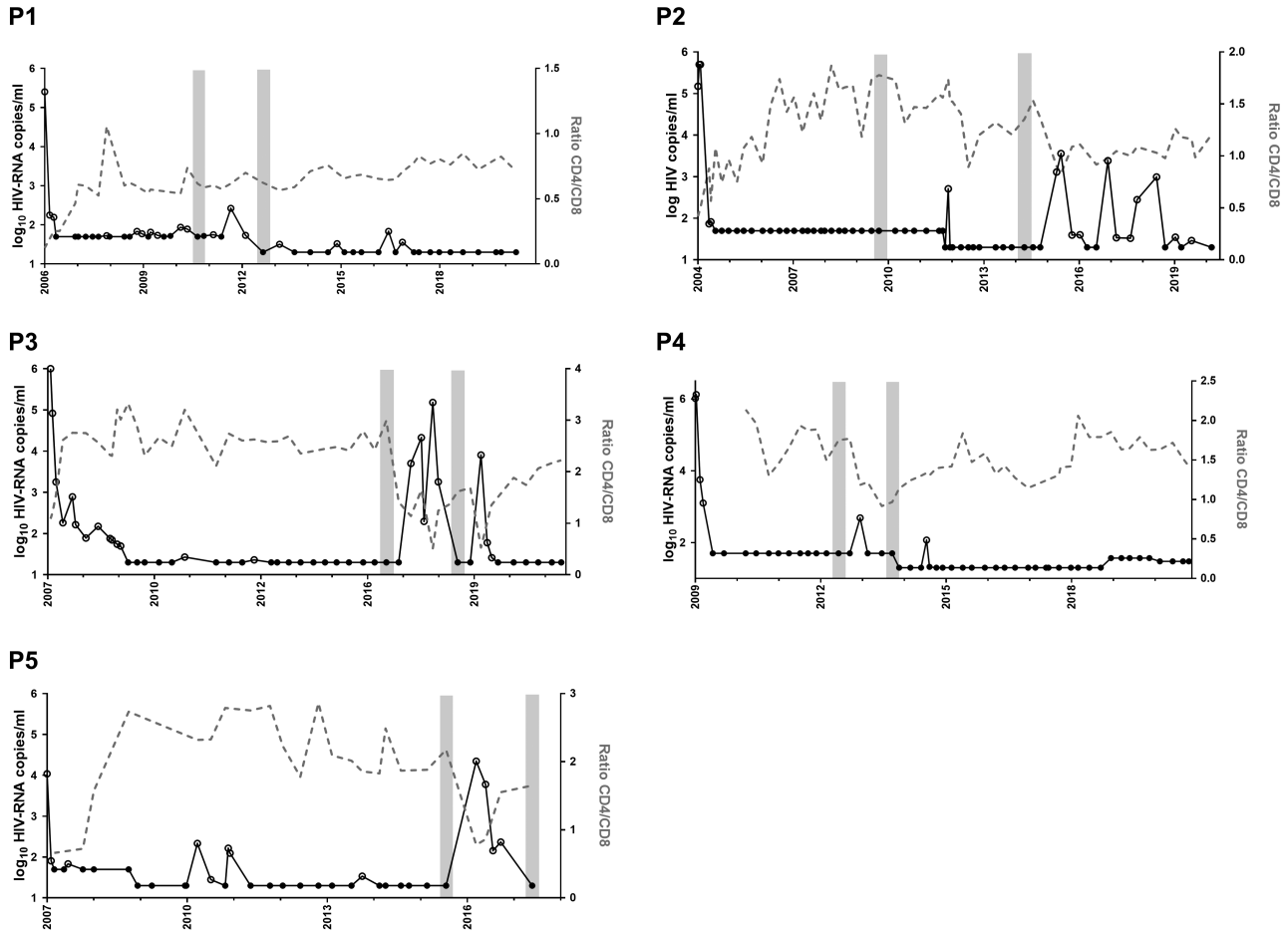

Figure 1. Plasma HIV-RNA viral load and ratio CD4/CD8 over time in children with perinatally acquired HIV-1 who develop transient viral rebounds (tVR). Open cycles represent viral load values above detection limit. Light gray bands are the time-points pre-loss (pre-tVR) and post-loss (post-tVR) selected for plasma multi-omic approaches. Note that, for both time-points, HIV viral load remains under detection limit (>20 copies/ml, but less than 1000 copies/ml) in all participants.

biomarkers of post-tVR time-point and reference group at sampling are shown in Table 2 and detailed ART-HIV regimens description from the reference group at sampling is shown in Supplementary Table 2. Children from the reference group had a median follow-up of 10 years [IQR: 8–13] and plasma HIV-RNA viral load, ratio CD4/CD8, and CD4-T cell count evolution over time per child are represented in Supplementary Figure 1. Children with PHIV with tVR had decreased nadir CD4 cell count compared with the reference group of children with PHIV with persistent viral control (393 [270–562] cells/mm^3 and 727 [435–966] cells/mm^3, respectively, $p = 0.072$) and also decreased %CD4+ (32.2% [23.8–39] and 42% [39–45.6], respectively, $p = 0.038$) and ratio CD4/CD8 at sampling (0.97 [0.77–1.63] and 1.83 [1.72–2.21], respectively, $p = 0.006$). Interestingly, children with tVR showed higher age at ART initiation compared with the reference group (36 [20–166] weeks and 7 [1.5–18.5] weeks, respectively, $p = 0.014$). Biochemical and inflammatory biomarkers at sampling including plasma glucose, glutamate pyruvate transaminase, glutamic oxaloacetic transaminase, total cholesterol, triglycerides, HDL, LDL, ratio LDL/HDL, and creatinine at sampling showed no differences between both groups.

A total of ten proteins were found significantly different between groups: the majority were downregulated (alpha-2-macroglobulin, apolipoprotein A-II, carboxylic ester hydrolase, apolipoprotein D, coagulation factor IX, peptidase inhibitor 16, and SAA2-SAA4 readthrough) and three of them upregulated (serotransferrin, clusterin, and kininogen-1 (KNG1)) on post-tVR time-point compared to the reference group of persistent viral control. The sparse partial least squares-discriminant analysis (sPLS-DA) confirmed that the majority of these proteins were the best discriminating on component 1, being serotransferrin and carboxylic ester hydrolase the key proteins differentiating both groups (Figure 2A).

The metabolomic analysis identified 8 metabolites with a significant increase or decrease in abundance comparing groups. Specifically, the levels of succinic acid, threonine, 2-hydroxyisovaleric acid, methionine, and 2-hydroxyglutaric

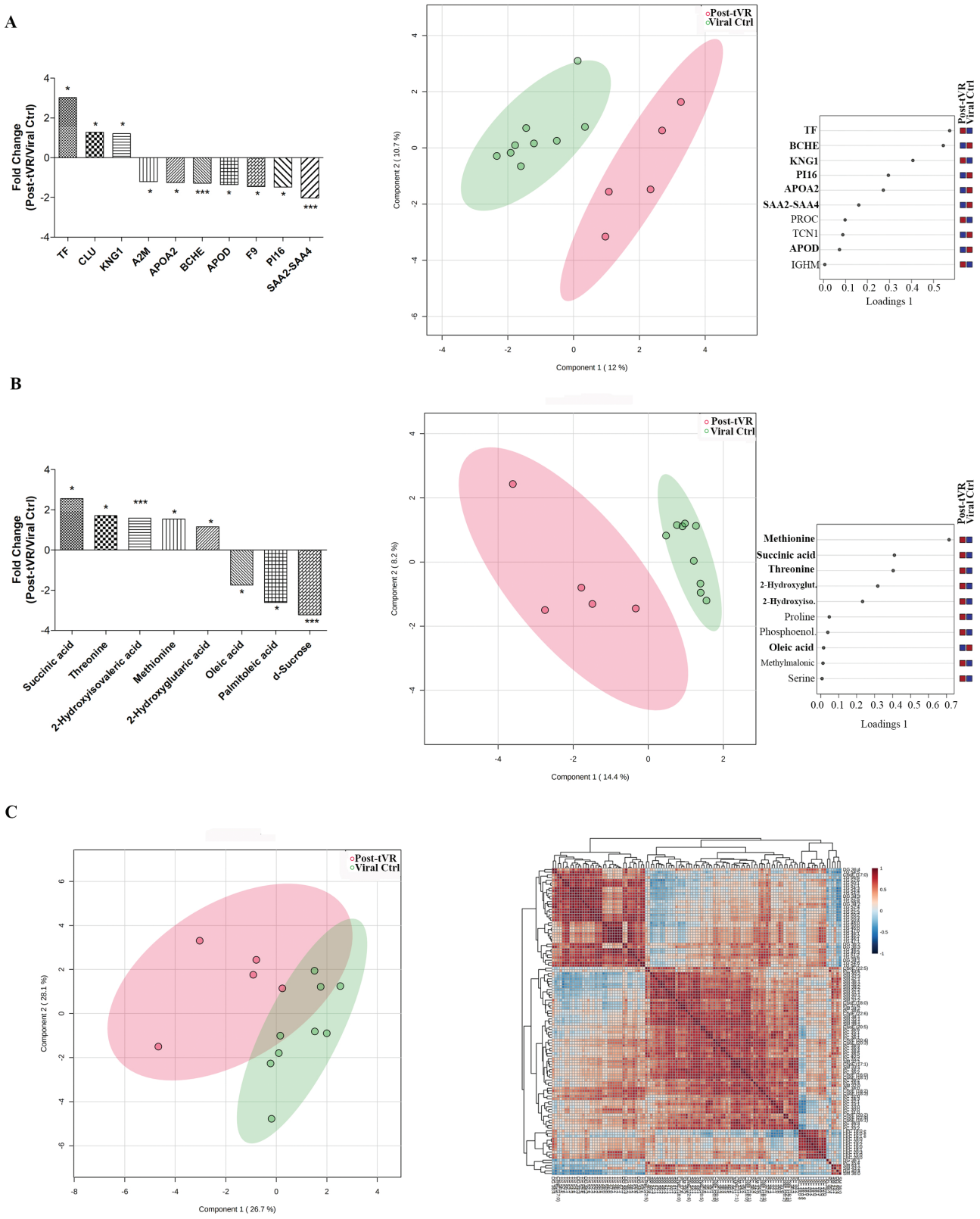

Figure 2. Multiomic analysis comparing post-tVR and reference group of children with perinatally acquired HIV-1 with persistent viral control. (A) Protein fold change of significantly changed proteins in post-tVR compared to the reference group (persistent viral control). Sparse partial least squares-discriminant analysis (sPLS-DA) plot displays the post-tVR group in red and the reference group with persistent viral control in green. Plot proteins loading graph insert displays key protein differences between groups for sPLS-DA component 1. (B) Metabolite fold change of significantly changed metabolites in post-tVR compared to the reference group (persistent viral control). sPLS-DA plot results on post-tVR and reference group, and plot metabolite loading graph (insert) displaying the key metabolite differences between groups for sPLS-DA component 1. (C) Loading score plots of sPLS-DA and correlation heatmap based on the 115 lipid species identified from the two groups under study. Spearman's coefficient values are depicted using the color gradient scale. *P value < 0.05, *** P value ≤ 0.001.

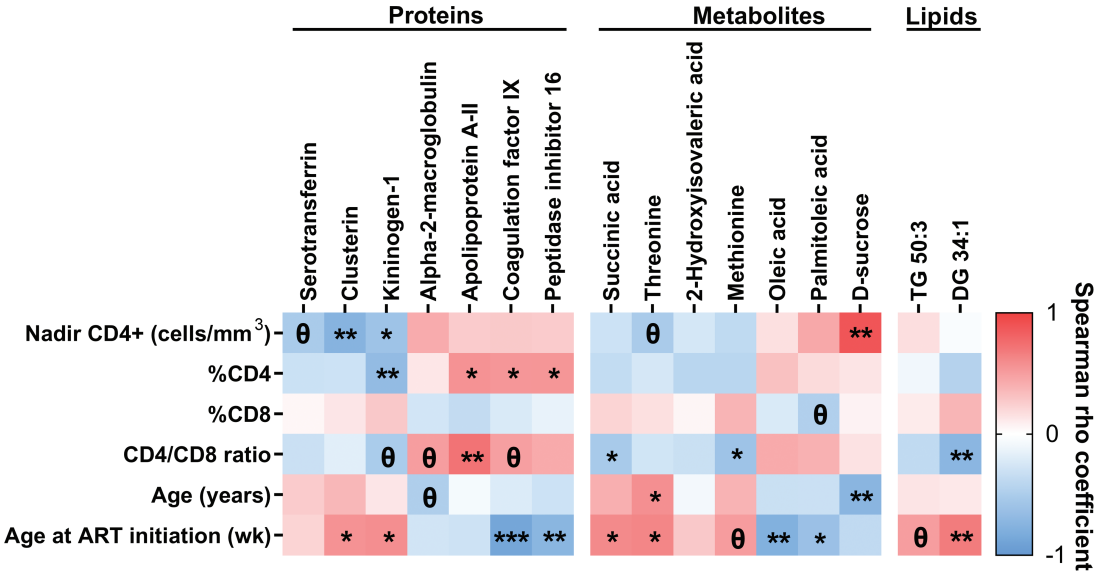

Figure 3. Correlations between proteins, lipids, and metabolites differentially expressed at post-tVR time-point and immunological and clinical parameters compared to the reference group. A total of 14 participants are included in the analysis. TG: triacylglyceride; DG: diacylglycerides; ART: antiretroviral treatment. The Spearman ρ correlation coefficient test was used. ϴ 0.1 > *P* value ≥ 0.05, **P* value < 0.05, ***P* value ≤ 0.01, ****P* value ≤ 0.001.

acid were significantly upregulated on post-tVR compared to the reference group. On the other hand, oleic acid, palmitoleic acid, and D-sucrose were downregulated. Again, sPLS-DA analysis revealed a clear separation comparing groups that was markedly defined by component 1 (Figure 2B). One triacylglyceride (TG 50:0) and one diacylglyceride (DG 34:1) were significantly upregulated after tVR compared to the reference group. Although no clear differentiation was observed on the sPLS-DA, in Spearman's correlation heatmap there were four groups of correlated marks identified (Figure 2C).

Correlation between Circulating Molecules with Age and Immunological Parameters

To ensure whether immunometabolic changes were a consequence of the viral rebound and address potential confounding factors such as the difference in age at ART initiation between groups, pre-tVR time-point from children with PHIV with tVR was also compared to the reference group of HIV-1 children with persistent viral control. The relative abundance of apolipoprotein D, SAA2-SAA4 readthrough, carboxylic ester hydrolase, and 2-hydroxyglutaric acid were already significantly different before tVR (pre-tVR) compared to the reference group with persistent viral control (data not shown), indicating that the previously described significant differences on these compounds between post-tVR and reference group, could not be explained as an effect of viral load increase and thus, they were excluded from following analyses.

To determine possible associations between the differentially expressed soluble markers and clinical parameters after tVR (post-tVR), the relative levels of the distinct proteins, lipids, and metabolites above identified were correlated with immunological parameters, age at ART initiation, and age at sampling in all participants (Figure 3). Ratio CD4/CD8 strongly correlated directly with soluble apolipoprotein A-II ($p = 0.004$; $\rho = 0.71$) and inversely with DG 34:1 and methionine ($p = 0.016$; $\rho = -0.63$ and $p = 0.032$; $\rho = -0.57$, respectively). Nadir CD4+ inversely correlated with clusterin and KNG1 levels ($p = 0.002$; $\rho = -0.758$ and $p = 0.022$; $\rho = -0.60$, respectively) and positively with D-sucrose ($p = 0.001$; $\rho = 0.77$). Age at ART initiation correlated positively and significantly with clusterin, KNG1, DG 34:1, succinic acid, and threonine ($p = 0.038$; $\rho = 0.56$; $p = 0.028$; $\rho = 0.58$, $p = 0.009$; $\rho = 0.671$, $p = 0.022$; $\rho = 0.60$; and $p = 0.017$; ρ=0.62, respectively) and inversely with coagulation factor IX, peptidase inhibitor 16, oleic acid, and palmitoleid acid ($p < 0.001$; $\rho = -0.878$, $p = 0.003$; $\rho = -0.73$, $p = 0.001$; $\rho = -0.78$, and $p = 0.016$; $\rho = -0.63$, respectively).

DISCUSSION

This study was designed to determine the immunometabolic changes associated with tVR with subsequent return to viral suppression in a cohort of children with PHIV by measuring soluble biomarkers by multi-omic approaches (proteomics, metabolomics, and lipidomics). The significant changes in several soluble compounds presented herein allowed us to deeper into the mechanisms that may be involved in the disease progression or development of comorbidities in children with PHIV who do not maintain persistent control of viremia.

In this study, we aimed to evaluate the consequences of tVR in a group of children with PHIV by comparing two paired

time-points being virally suppressed: before and after the first episode of tVR during the follow-up. Alterations in ART adherence and viral failure have been associated with high levels of inflammation and immune activation independently of plasma HIV RNA suppression [5]. However, the low statistical power and the number of participants in our study could explain the lack of significant differences in the paired comparisons between pre- and post-tVR time-points.

In the comparison of children with PHIV and tVR and the reference group of children with PHIV with persistent viral control, the soluble levels of apolipoprotein D, SAA2-SAA4 readthrough, carboxylic ester hydrolase, and 2-hydroxyglutaric acid were already significantly different before the tVR. Thus, it is plausible that in our study, the participants that developed viral loss of control due to ART failure or poor adherence might show already at pre-tVR time-point altered soluble variables despite apparent virologic suppression due to low-level residual plasma viremia. This supports the premise that incomplete adherence, even if sufficient to maintain viral suppression, might imply low-level inflammation with detrimental consequences such as increased frequency of comorbidities as has been previously described [22]. Another documented explanation could be the differences in age at ART initiation among groups. The age at ART initiation was not considered a matching variable but the reference group of children with PHIV with persistent viral control showed an early age at ART introduction. The results could be in agreement with previous studies in which our group identified soluble profiles of proteins and miRNAs based on ART delay in PHIV infected patients [21, 23].

Current guideline recommendations indicate that tVR and blips can safely be monitored without the need to alter the antiretroviral regimen. Most of the studies for monitoring tVR have been focused on adults but children and adolescents are potentially at higher risk of developing viremia due to weight-based, dosing and variable drug levels, poor tolerability of drugs, and suboptimal adherence. The results presented herein suggest that children with PHIV and tVR enrolled in our study may benefit from closer clinical monitoring due to the reduction in the ratio CD4/CD8 that the tVR implied. The coefficient value below 1 is considered a prognostic marker of mortality and non-AIDS defining events together with CD4-T cell count evolution among long-term virologically suppressed HIV patients [24–26]. Interestingly, after tVR, the correlations observed between ratio CD4/CD8 and CD4-T cell counts with proteins like KNG1 and lipids such as DG 34:1, reinforce the importance of ratio CD4/CD8 as a marker of immune dysfunction to identify patients at higher risk of long-term complications and give evidences about the possible mechanism involved. Of note, the overexpression of KNG1 stands out due to its association with early cognitive impairment in the general population as well as diabetic nephropathy [27, 28].

Although the distinct soluble compounds that were already significantly different before the tVR were excluded for the analysis of associations with immunological and clinical variables, several soluble biomarkers strongly correlated with age at ART initiation. Due to the tight correlation between HIV reservoir and age at ART initiation [29–31] and, as transient viral replication implies an increase in HIV reservoir, the associations observed with age at ART initiation may reflect a probably augment in the reservoir on those participants with a viral rebound. However, in our cohort, we had no data related to the HIV reservoir, which is one of the main limitations.

Moreover, our data indicated that an increase in circulating KNG1 directly correlated with the age at ART initiation but at the same time, it was inversely related to low CD4-T cell counts. Thus, an ART delay, and therefore a high HIV viral reservoir in PHIV patients, could be related not only to an immune function impairment but also to potential early cognitive impairment, as mentioned above.

The limitations of the study include the relatively small sample size in each group, and there may, therefore, be inadequate power to detect associations between soluble markers and the immunological variables and future clinical progression. This limitation is counterbalanced by the value of this cohort, a longitudinal study of PHIV patients with a delayed standard of care. Additionally, children with PHIV were very heterogeneous in terms of the causes of tVR and anti-HIV ART regimens. Due to this limitation, we could not inquire deeply into the possible impact of the different ART used. However, as strengths, patients included in this study have exhaustive follow-up and detailed clinical data including adherence data and non-AIDS-events occurrences that will help us to determine in the future if distinct soluble markers could evolve in clinical consequences.

In conclusion, this study shows that transient loss of viral control followed by suppression deals with significant changes in soluble proteins, lipids, and metabolites that correlated with immunological parameters, mainly ratio CD4/CD8, traditionally associated with disease progression in HIV infection, that remains inverted in the group of children with PHIV after tVR. In this sense, the distinct soluble biomarkers described herein could be considered potential biomarkers of immune progression and future investigations will determine their possible role in the development of future non-AIDS-events in pediatric HIV-1 population.

Supplementary Data

Supplementary materials are available at the *Journal of The Pediatric Infectious Diseases Society* online (http://jpids.oxfordjournals.org).

Notes

Financial support. This work was supported by the Fondo de Investigacion Sanitaria [PI19/01337 and PI20/00326]-ISCIII-FEDER (co-funded by the European Regional Development Fund/European Social

Fund; "A way to make Europe"/"Investing in your future"); Programa de Suport als Grups de Recerca AGAUR (2017SGR948); and The SPANISH AIDS Research Network [RD16/0025/0006 and RD16/0025/0019]-ISCIIIFEDER (Spain), the Spanish Pediatric HIV Network (CoRISpe) integrated in the Spanish National AIDS Network (RIS-EPICLIN-06/2017), the Centro de Investigación Biomédica en Red de Enfermedades Infecciosas-ISCIII [CB21/13/00020, CB21/13/00025, CB21/13/00077], and the Bioingenieria, Biomateriales y Nanomedicina [CB22/01/00041], Madrid, Spain. FV is supported by grants from the Programa de Intensificacion de Investigadores (INT20/00031)-ISCIII and by "Premi a la Trajectoria Investigadora dels Hospitals de l'ICS 2018." AR is supported by IISPV through the project "2019/IISPV/05" (Boosting Young Talent), by GeSIDA through the "III Premio para Jovenes Investigadores 2019" and by "CP19/00146" through the Miguel Servet Program. LT-D by the Instituto de Salud Carlos III (ISCIII) under grant agreement "CD20/00025" through the Sara Borrell Program and by GeSIDA through the "IV Premio para Jovenes Investigadores 2021."

Potential conflicts of interest. The authors declare no conflict.

Acknowledgments. This study would not have been possible without the generous collaboration of all the patients and their families and medical and nursing staff who have taken part in the project. We also thank Antoni del Pino and Salvador Fernandez-Arroyo from the Proteomics and Metabolomics facilities of the Centre for Omic Sciences (COS) Joint Unit of the Universitat Rovira i Virgili-Eurecat for their contribution to mass spectrometry analyses.

Transparency declarations. None to declare.

References

1. Cohen Stuart JW, Wensing AM, Kovacs C, et al. Transient relapses ("blips") of plasma HIV RNA levels during HAART are associated with drug resistance. *J Acquir Immune Defic Syndr* **2001**; 28:105–13.
2. Podsadecki TJ, Vrijens BC, Tousset EP, Rode RA, Hanna GJ. Decreased adherence to antiretroviral therapy observed prior to transient human immunodeficiency virus type 1 viremia. *J Infect Dis* **2007**; 196:1773–8.
3. Jones L, Perelson A. Opportunistic infection as a cause of transient viremia in chronically infected HIV patients under treatment with HAART. *Bull Math Biol* **2005**; 67:1227–51.
4. Fleming J, Mathews WC, Rutstein RM, et al; HIV Research Network. Low-level viremia and virologic failure in persons with HIV infection treated with antiretroviral therapy. *AIDS* **2019**; 33:2005–12.
5. Castillo-Mancilla JR, Brown TT, Erlandson KM, et al. Suboptimal adherence to combination antiretroviral therapy is associated with higher levels of inflammation despite HIV suppression. *Clin Infect Dis* **2016**; 63:1661–7.
6. Fidler S, Olson AD, Bucher HC, et al. Virological blips and predictors of post treatment viral control after stopping ART started in primary HIV infection. *J Acquir Immune Defic Syndr*. **2017**; 74:126–33.
7. Young J, Rickenbach M, Calmy A, et al. Transient detectable viremia and the risk of viral rebound in patients from the Swiss HIV Cohort Study. *BMC Infect Dis*. **2015**; 15:382.
8. Kanapathipillai R, Mcmanus H, Cuong D, et al. The significance of low-level viraemia in diverse settings: analysis of the Treat Asia HIV Observational Database (TAHOD) and the Australian HIV Observational Database (AHOD). *HIV Med* **2014**; 15:406–16.
9. Taiwo B, Hunt PW, Gandhi RT, et al. CD8+ T-cell activation in HIV-1-infected patients experiencing transient low-level viremia during antiretroviral therapy. *J Acquir Immune Defic Syndr* **2013**; 63:101–4.
10. Castro P, Plana M, González R, et al. Influence of episodes of intermittent viremia ("Blips") on immune responses and viral load rebound in successfully treated HIV-infected patients. *AIDS Res Hum Retroviruses* **2013**; 29:68–76.
11. Hermankova M, Ray SC, Ruff C, et al. HIV-1 drug resistance profiles in children and adults with viral load of < 50 copies/mL receiving combination therapy. *JAMA* **2001**; 286:207.
12. Pereira R, Ludwig DA, Mathew S, et al. Predicting viral failure in human immunodeficiency virus perinatally infected youth with persistent low-level viremia on highly active antiretroviral therapy. *J Pediatric Infect Dis Soc* **2019**; 8:303–9.
13. Sudjaritruk T, Aurpibul L, Ly PS, et al. Incidence of post-suppression virologic rebound in perinatally HIV-infected Asian adolescents on stable combination antiretroviral therapy. *J Adolesc Health* **2017**; 61:91–8.
14. Shiau S, Abrams EJ, Arpadi SM, Kuhn L. Early antiretroviral therapy in HIV-infected infants: can it lead to HIV remission? *Lancet HIV* **2018**; 5:e250–8.
15. Farmer A, Wang X, Ganesan A, et al. Factors associated with HIV viral load "blips" and the relationship between self-reported adherence and efavirenz blood levels on blip occurrence: a case-control study. *AIDS Res Ther* **2016**; 13:16.
16. De Scheerder M-A, Van Hecke C, Zetterberg H, et al. Evaluating predictive markers for viral rebound and safety assessment in blood and lumbar fluid during HIV-1 treatment interruption. *J Antimicrob Chemother* **2020**; 75:1311–20.
17. Guo H, Wang Q, Ghneim K, et al. Multi-omics analyses reveal that HIV-1 alters CD4+ T cell immunometabolism to fuel virus replication. *Nat Immunol* **2021**; 22:423–33.
18. Angin M, Volant S, Passaes C, et al. Metabolic plasticity of HIV-specific CD8+ T cells is associated with enhanced antiviral potential and natural control of HIV-1 infection. *Nat Metab* **2019**; 1:704–16.
19. Jose MI de, Jiménez de Ory S, Espiau M, et al. A new tool for the paediatric HIV research: general data from the Cohort of the Spanish Paediatric HIV Network (CoRISpe). *BMC Infect Dis* **2013**; 13:2.
20. Garcia-Merino I, Las Cuevas N de, Jimenez JL, et al. Pediatric HIV BioBank: a new role of the Spanish HIV BioBank in pediatric HIV research. *AIDS Res Hum Retroviruses*. **2010**; 26:241–4.
21. Tarancón-Diez L, Rull A, Herrero P, et al. Early antiretroviral therapy initiation effect on metabolic profile in vertically HIV-1-infected children. *J Antimicrob Chemother* **2021**; 76:2993–3001.
22. Castillo-Mancilla JR, Cavassini M, Schneider MP, et al; Swiss HIV Cohort Study. Association of incomplete adherence to antiretroviral therapy with cardiovascular events and mortality in virologically suppressed persons with HIV: the Swiss HIV Cohort Study. *Open Forum Infect Dis* **2021**; 8:ofab032.
23. Tarancon-Diez L, Consuegra I, Vazquez-Alejo E, et al. miRNA profile based on ART delay in vertically infected HIV-1 youths is associated with inflammatory biomarkers and activation and maturation immune levels. *Front Immunol* **2022**; 13:878630.
24. Han J, Mu W, Zhao H, et al. HIV-1 low-level viremia affects T cell activation rather than T cell development in school-age children, adolescents, and young adults during antiretroviral therapy. *Int J Infect Dis* **2020**; 91:210–7.
25. Pollock KM, Pintilie H, Foster C, Fidler S. Cross-sectional study of CD4: CD8 ratio recovery in young adults with perinatally acquired HIV-1 infection. *Medicine (Baltimore)* **2018**; 97:e9798.
26. Carrasco I, Tarancon-Diez L, Vázquez-Alejo E, et al. Innate and adaptive abnormalities in youth with vertically acquired HIV through a multicentre cohort in Spain. *J Int AIDS Soc* **2021**; 24:e25804.
27. Markaki I, Bergström S, Tsitsi P, et al. Cerebrospinal fluid levels of Kininogen-1 indicate early cognitive impairment in Parkinson's disease. *Mov Disord* **2020**; 35:2101–6.
28. Na Nakorn P, Pannengpetch S, Isarankura-Na-Ayudhya P, et al. Roles of kininogen-1, basement membrane specific heparan sulfate proteoglycan core protein, and roundabout homolog 4 as potential urinary protein biomarkers in diabetic nephropathy. *EXCLI J* **2020**; 19:872–91.
29. Martínez-Bonet M, Puertas MC, Fortuny C, et al. Establishment and replenishment of the viral reservoir in perinatally HIV-1-infected children initiating very early antiretroviral therapy. *Clin Infect Dis* **2015**; 61:1169–78.
30. Persaud D, Gay H, Ziemniak C, et al. Absence of detectable HIV-1 viremia after treatment cessation in an infant. *N Engl J Med* **2013**; 369:1828–35.
31. Tagarro A, Chan M, Zangari P, et al. Early and highly suppressive antiretroviral therapy are main factors associated with low viral reservoir in European perinatally HIV-infected children. *J Acquir Immune Defic Syndr* **2018**; 79:269–76.